Optical Pump-Terahertz Probe Spectroscopy of Condensed Phase Reaction Dynamics

Bret N. Flanders and Norbert F. Scherer*

Department of Chemistry and The James Franck Institute, University of Chicago, 5735 S. Ellis Ave. Chicago, IL

*Author to whom correspondence should be addressed

Abstract

The general theoretical and experimental principles of optical pump-THz probe spectroscopy of chemical reactions in liquids is presented. Background on specific difficulties encountered in the experimental observation is reviewed. Chiefly, signal-to-noise ratios currently limit the quality of information that can be extracted from optical pump-THz probe data on chemical reactions. This issue is shown to be connected to the assumption of linear response. The problem of interpretation of frequency dependent absorption coefficient data of neat liquids and solutions is addressed, and reasonably successful methods for analysis of the data are presented. Transient absorption coefficient spectra of <111> GaAs illustrates the type of information this spectroscopic method can extract from condensed phase samples.

1. Introduction

Theoretical and experimental elucidation of the physical processes that occur on the molecular level in liquids has occupied the efforts of physicists and chemists for most of the century.[1] Langevin's 1908 equation of Brownian motion is used today, albeit in modified form, to describe the motion of a tagged molecule in a condensed phase environment. Furthermore, Debye's 1929 treatise on polar liquids provides the standard physical description of rotational diffusion in liquids. The Onsager regression hypothesis of 1930 functioned as the cornerstone for the non-equilibrium statistical mechanical theories of liquids that have since followed. In 1960, building on the theory of linear response set forth by Kubo in the 1950's, Zwanzig formulated a generalized form of the Langevin Equation. The significance of this advancement lies in the re-expression of the bath forces on a tagged particle as a sum of a neat bath term, and a memory term. This latter term connects the complex motion of a particle's past to the present behavior of that particle. It is the interaction with the many surrounding molecules of the liquid solvent that dictates the time scale of this memory effect. The consequence of memory is a frequency dependent as opposed to a static or zero-frequency friction function.

With the advent of ultrafast spectroscopy in the 1980's the experimental tools for observation of friction in liquids became available. Two techniques have since come to the forefront in the effort to cleanly observe relaxation processes in liquids: Time-dependent fluorescence Stokes-shift spectroscopy and optical pump-THz probe spectroscopy. In the former method, which yielded the first observation of frequency dependent friction,[2,3] the fluorescence of a solvated dye molecule is observed as a function of time. The change in the color of the fluorescence (red-shift) reflects the changing solvent environment from which the dye molecule emits. As these solvent molecules reorganize into a configuration favorably aligned with the solute's new dipole moment, the excited electronic state-ground electronic state free energy difference is reduced; hence the red-shift in the fluorescence. Thus, solvent reorganization is observed somewhat vicariously through frequency resolution of the fluorescence from the solute. Information on the solvent reorganization process is, therefore, inferred. Conversely, an important value of optical pump-THz probe studies is the ability to observe the solvent directly. In an intramolecular charge transfer reaction with a corresponding solute dipole moment change, the surrounding solvent molecules are initially in a configuration of favorable alignment with the electric field of the ground state solute dipole moment.[3] Following an optically induced excitation, the surrounding solvent molecules move (via translations and rotations) in a complex way in order to achieve a new configuration that is equilibrated to excited state solute dipole moment.[4,5]

The determination of the magnitudes and time scales of the motions undergone during this reorganization process is a primary goal in the effort to understand the physical details of reactions in liquids. Often the rotational and translational modes that are involved in the reorganization of the solvent about the new solute charge distribution are of very low frequency, absorbing radiation in the 0 to 120 cm^{-1} region of the electromagnetic spectrum. Hence, pulsed terahertz spectroscopy, sensitive to dipolar absorption of radiation in the 3 to 120 cm^{-1} spectral range, is a suitable method for the study of these solvent motions. Assuming the validity of linear response, the fluctuation-dissipation theorem provides a starting point for using the equilibrium spectrum, obtainable from steady-state pulsed THz spectroscopy, to model the solvent response to a chemical reaction.[6,7,8] Hence, the determination of these equilibrium solvent dynamics is directly related to knowing the solvent modes involved in a non-equilibrium situation, such as a chemical reaction. Therefore, significant effort has been spent on understanding the molecular processes that give rise to the steady-state absorption coefficient spectrum. However, even more fundamental information lies in the optical pump-THz probe measurement. That is, detection of the non-equilibrium solvent response to a charge transfer on the solute would provide an experimental means of assessing the validity of linear response through the direct comparison of the measured non-equilibrium and equilibrium spectra. This knowledge is of fundamental and practical importance since nearly all theories of liquids employ this assumption.

2. Model of Problem

The theoretical foundation of the proposed optical pump-THz probe study is well known.[5] An illustration of this process of reaction induced solvent reorganization is shown in Figure 1. The salient points of this classical theory are presented here. One can think of the optical excitation of the solute as the turning off of the ground state dipole moment and the simultaneous turning on of the excited state dipole moment. Each has an electric field associated with it. Hence, the reorganization of surrounding solvent molecules is a relaxation from the "non-equilibrium" configuration characterized by alignment with the ground state electric field to an "equilibrium" one in alignment with the excited state electric field.[9]

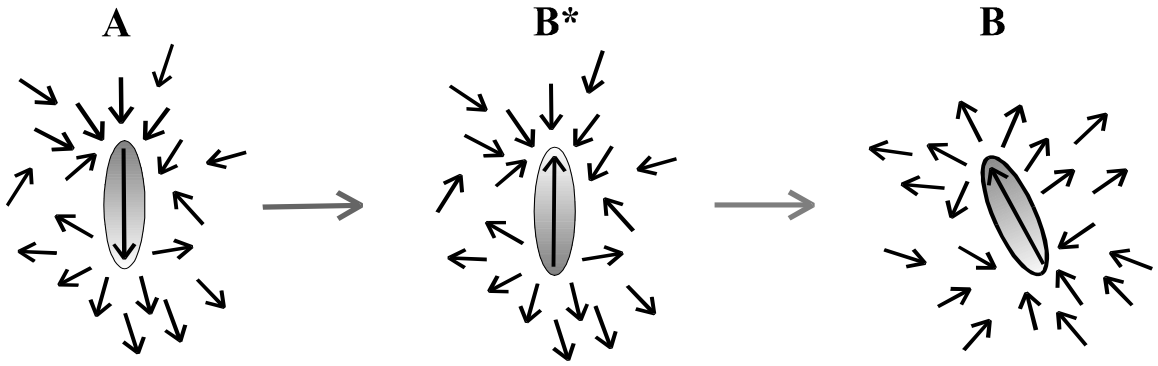

Mathematically, the perturbation may be expressed as

$$\Delta H = -\vec{M} \cdot \Delta\vec{E} \qquad \textbf{(1)}$$

where M is the solvent polarization. This quantity is the experimental observable in pulsed THz absorption measurements and is calculated by summing over the individual vector dipole moments, μ_i, of the solvent molecules

$$\vec{M} = \sum_{i}^{solvent} \vec{\mu}_i \qquad \textbf{(2)}$$

where the sum runs over the surrounding solvent molecules. The quantity $\Delta\overline{E}$ in Eqn. (1) is the effective electric field due to the removal of the ground state solute dipole moment electric field and the addition of that due to the excited state dipole moment. Therefore, the effective E-field felt by the solvent after optical

excitation (*i. e.* at t>0) is the difference between the E-fields of the ground and excited states of the solute molecule. That is, $\Delta\vec{E}$ reduces to

$$\Delta\vec{E} = \frac{\Delta\mu}{4\pi\varepsilon_0 r^2} \tag{3}$$

where $\Delta\mu = \mu_e - \mu_g$. The radial variable, r the distance between the center of mass of the solute and the center-of-mass of a bath molecule.

The time dependence of ΔH reflects the step function nature of the optical excitation. The physical quantity that pulsed terahertz spectroscopy measures is the solvent polarization M(t). At t=0, the instant of impulsive solute excitation, the non-equilibrium value of the polarization $\overline{M}(0)$ and the corresponding solvent configuration are identical to the equilibrium value <M> and solvent configuration for times before t=0. Note that pointed brackets <M> denote the equilibrium ensemble averaged value of the variable M whereas the horizontal bar $\overline{M}$(t) denotes non-equilibrium average value of the variable M Furthermore, the equilibrium fluctuation of a variable M(t) will be denoted

$$\delta\vec{M}(t) = \vec{M}(t) - \langle M \rangle \tag{4a}$$

And the non-equilibrium displacement of a variable M(t) is expressed as

$$\Delta\vec{M}(t) = \overline{M}(t) - \langle M \rangle \tag{4b}$$

The non-equilibrium value $\overline{M}$(t) may be expressed as[5]

$$\overline{M}(t) = \frac{Tr\left[F(r^N, p^N)M(t)\right]}{Tr\left[F(r^N, p^N)\right]} \tag{5a}$$

$$= \frac{Tr\left[\exp\left(-\beta(H+\Delta H)\right)M(t)\right]}{Tr\left[\exp\left(-\beta(H+\Delta H)\right)\right]} \tag{5b}$$

where $F(r^N,p^N)$ is the non-equilibrium phase space distribution function which is proportional to $e^{-\beta(H+\Delta H)}$ and $\beta=(k_BT)^{-1}$ The expansion about ΔH in the expression for the non-equilibrium average of the solvent polarization, $\overline{M}$(t), is logical because the non-equilibrium state of the system is due to the perturbation ΔH. Assuming that ΔH is small, a series expansion of the $e^{-\beta\Delta H}$ factor in Eqn. (5b) may be truncated after the second term such that

$$\overline{M}(t) = \frac{Tr\left[\exp\left(-\beta H\right)\left(1-\beta\Delta H\right)M(t)\right]}{Tr\left[\exp\left(-\beta H\right)\left(1-\beta\Delta H\right)\right]} \tag{6}$$

After some algebraic manipulation, and the additional assumption that $1/(1-x) \cong 1+x$ where x is proportional to βΔH (again, valid in the limit of small βΔH), $\overline{M}$(t) may be simplified to

$$\overline{M}(t) = \langle M \rangle - \beta\langle \Delta H \cdot M(t) \rangle + \beta\langle M \rangle\langle \Delta H \rangle + O\left((\beta\Delta H)^2\right) \tag{7}$$

On substitution of Eqn. (1) for ΔH, and use of Eqn. (4b) for $\Delta\overline{M}$(t) the following expression for the non-equilibrium displacement of the polarization from its equilibrium values is obtained:

$$\Delta\overline{M}(t) = \beta\Delta\vec{E}\langle \vec{M} \cdot \vec{M}(t) \rangle - \beta\Delta\vec{E}\langle \vec{M} \rangle^2 + O\left(\Delta\vec{E}^2\right) \tag{8}$$

Use of expression (4a) for an equilibrium fluctuation about <M>, and employing the (perhaps incorrect) assumption that the terms nonlinear in $\Delta\overline{E}$ are negligible, Eqn. (6) may be re-written as

$$\Delta\overline{M}(t) = \beta\Delta\vec{E}\langle\delta M \cdot \delta M(t)\rangle \quad \textbf{(9)}$$

This equation is the fluctuation-dissipation theorem. The significance of this general result to optical pump-THz probe studies lies in the assumption that βΔH is small. In that case, one can expect to observe non-equilibrium relaxation that is a linear function of the equilibrium dipole moment time correlation function as expressed in Eqn. (9). However, ΔH is proportional to Δμ, so a solute molecule with a large enough dipole moment change upon excitation will drive the solvent response out of the linear regime. From an experimental standpoint, one chooses the solute-solvent system such that Δμ is large for the sake of obtaining observable signal. Indeed, the low signal-to-noise ratios observed in the few optical pump-THz probe studies reported thus far (on beatine-30 in chloroform[10], on betaine-30 in dichlorobenzene (DCB)[11] and para-nitroaniline in DCB[11]) indicate that a large perturbation is, if not necessary, certainly desirable. However, even if it is determined that good experimental data can only be obtained when there is appreciable nonlinear solvent response, the establishment of an upper bound for Δμ would be of value.

Figure 1 illustrates this process of solvent reorganization. In the illustrated case, the solute dipole is exactly reversed on excitation from the ground to the excited state. Therefore, with $\mu_e = -\mu_g$, and the value of $\Delta\mu = -2\mu_g$, with a corresponding electric field. For this simple example, the calculation of the interaction energy between the dipolar solute and the surrounding solvent molecules is straightforward. This quantity is merely the negative dot product of the solvent polarization and the solute E-field. That is,

$$U(t) = -\vec{M}(t)\cdot\Delta\vec{E}(t) \quad \textbf{(10a)}$$

$$= -\vec{M}(t)\cdot\frac{\Delta\vec{\mu}(t)}{4\pi\varepsilon_0 r^2} \quad \textbf{(10b)}$$

The second equality was obtained through substitution of Eqn. (3) for $\Delta\overline{E}$. Furthermore the solvent polarization, and the difference between solute dipole vectors have been written as functions of time. The solute E-field time dependence depends on the degree to which the solute rotates after optical excitation, that is, in moving from B^* to B in Figure 1. M(t) changes in a complicated manner since its value depends on the instantaneous orientations of many solvent molecules. Immediately following excitation the solvent has not yet begun to reorganize, and the interaction energy is at a maximum. The total (outer sphere) reorganization energy may then be calculated. At t=0, cos(θ, t=0) =-1 because M(0) and $\Delta\overline{E}(0)$ directly oppose each other. Therefore, the dot product in Eqn. (10b) simplifies to

$$U(0) \propto \left|\Delta\vec{\mu}\right|\left|\vec{M}\right| \quad \textbf{(11a)}$$

$$\propto 2\left|\vec{\mu}_g\right|\left|\vec{M}\right| \quad \textbf{(11b)}$$

where the second equality was obtained from the relationship $\Delta\mu = -2\mu_g$ for the case pictured in Figure 1, and this is the quantity of energy that is dissipated amongst the bath molecules during the relaxation of the system from B^* to B.

3. Experimental

While the first optical pump-FIR probe experiment was performed a decade ago[12], and a handful of such studies have since been reported,[13,14,15] and the first *comprehensive* study of a reactive liquid solution still lies in the (near)[10,11] future. Some requirements for the optimal construction of such a spectrometer may be stated. Foremost in importance is the development of a THz pulse generation and detection system that is sensitive enough to detect the optical pump-induced response. Second, an intense optical pump source capable of initiating a large non-equilibrium response such as a chemical reaction must be available. Finally, pulse-train repetition rates lower than the excited state decay rate of the e.g. solute molecule are necessary. A cavity-dumped pulse-driven terahertz spectrometer has been constructed whose performance satisfies the above requirements. A description of this instrument is given here, but a more complete account may be found elsewhere.[16]

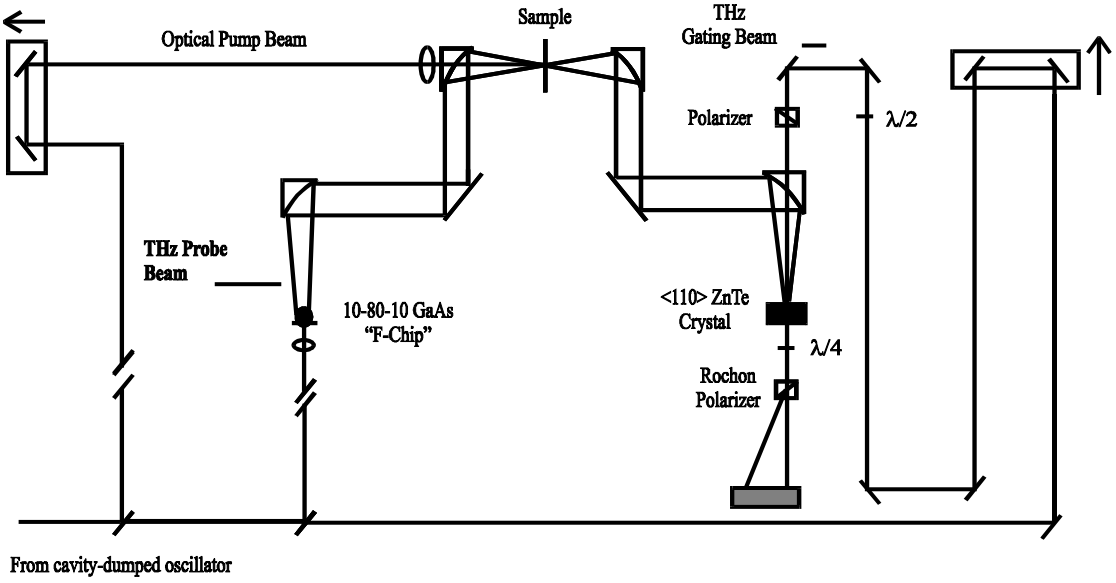

Figure 2: Optical pump-THz Probe Spectrometer.

Cavity-dumping a high rep-rate oscillator allows an increase in pulse energy and provides control over the repetition rate of the emitted pulses. The home-built cavity-dumped ti:sapphire (CD-TS) oscillator operates without additional noise (relative to the mode locked output) in the cavity-dumped pulse train. A detailed description of the home-built oscillator system is given elsewhere.[17] The output of the CD-TS laser, characterized by a 250kHz pulse train delivering 15mW average power and 60nJ pulse energy, was directed into the optical pump-THz probe spectrometer (illustrated in Figure 2).

In this experimental configuration, a 50/50 pellicle beam splitter is used to direct a portion of the main beam onto the first time delay stage for the purpose of introducing a large perturbation in the sample. This stage delays the arrival of the optical pump pulse relative to the arrival time of the peak of the THz probe pulse. The optical power in this pump beam is typically 4.0mW and, thereby delivers a 16nJ pulse to the sample. A 2.5" f.l. doublet lens is used to focus the pump beam through a 2.0mm hole along the optical axis of the Au coated paraboloid into the sample. Corrections in the position of the pump beam on the sample may be made through small translations of this lens. The transmitting antenna structure, described in detail elsewhere,[18] is composed of two 10μm gold transmission lines on a GaAs wafer. The separation between the parallel lines is 80μm and a +65V bias is applied to the transmitter. The 0.8mW of 790nm ti:sapphire radiation is focused through a f =

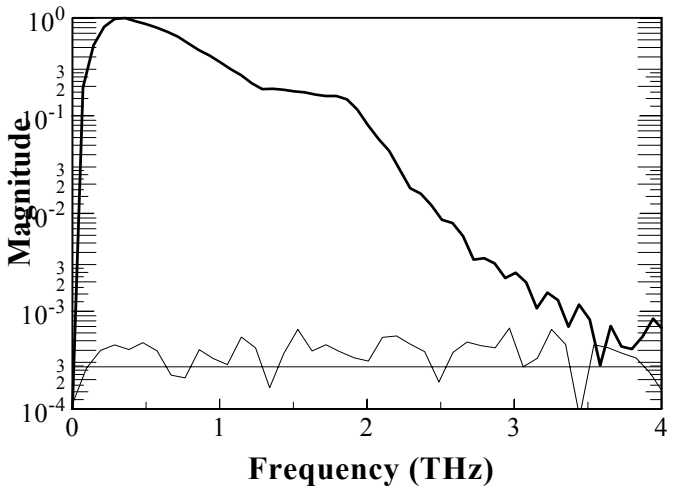

Figure 3: The magnitude spectrum of the THz pulse is shown in bold. The noise spectrum, measured by blocking the THz source excitation beam, is the light solid line. The constant line at magnitude of 2.4 X10^{-4} is included as a guide to the eye.

2.5cm diode doublet lens onto the "F-chip" source producing a sudden population of carriers in the region of the GaAs between the two transmission lines. The GaAs is irradiated with a defocused optical beam (diameter ~50μm) to prevent premature circuit burnout by the excessive current in the antenna generated by the focused cavity-dumped pulse. The approximately half toroidal volume of THz radiation emitted from the back side of the GaAs wafer is collected by a high resistivity Si lens. A paraboloidal-flat-paraboloidal combination of Au-coated mirrors is used to collimate, direct and focus the beam of THz pulses into the sample, respectively. A similar combination of optics is used to collect, direct and focus the THz beam into the 1.5mm thick <111> ZnTe electro-optic sensor, where the THz signal is detected by the Pockel's effect.[19]

Figure 3 illustrates the measured THz pulse magnitude spectra (in bold) obtained without a sample present. The spectra result from Fourier-transformation of the measured temporal profiles (not shown). The optical gating beam passes through the ZnTe EO sensor, a λ/4 plate and a rochon polarizer and is incident on the balanced photo-receiver. The signal-to-noise ratio of the resulting averaged pulse is 6300. The lighter trace in Figure 3 represents the noise spectrum of the detection system in the terahertz spectrometer. For this measurement, the bias across the antenna was removed and the optical beam incident on the THz source was blocked in order to block the rectified THz field. Only the probe beam still illuminated the detection optics and photodiodes. An average of six-7ps scans was acquired, as in the previous measurement of the THz pulse, and was Fourier transformed to give the noise spectrum. The noise floor for this THz spectrometer lies at 2.7×10^{-4} allowing nearly four decades of dynamic range. This has been shown to exceed the dynamic range of THz pulses generated in output coupled (high rep-rate) oscillator-driven THz spectrometers.[14]

4. Steady-State Pulsed THz Studies of Liquids

The generalized Langevin Equation provides the connection between the complicated decay of the dipole time correlation function and the concept of a time dependent, or upon Fourier transformation, a frequency dependent friction. In the simplest Markovian case, this friction is static because the correlation time for the fluctuating forces in the bath is assumed to be instantaneous on the time scale of the observation. Therefore, the memory term in this limit is non-zero at only one time. However, dipole moment time correlation functions that are measurable in the absorption coefficient studies of pulsed THz spectroscopy decay on time scales comparable to the intrinsic correlation times of the bath. Therefore, non-Markovian dynamics are relevant to the analysis of this far-infrared (FIR) absorption coefficient data. Two methods of analysis are presented below. Both attempt to account for the intermolecular interactions in absorbing liquids in a quantitative way for the purpose of decomposing the typically featureless absorption spectra that is observed in the FIR spectral region of liquids.

4.1 The Mori formalism for expressing the dipole moment TCF of $CHCl_3$, CCl_4 and their mixtures

The Mori line shape function formalism provides a successful method for fitting the dipole moment time correlation function (DMTCF) (or more specifically the frequency dependent absorption coefficient) measured by pulsed THz spectroscopy on weakly polar and nonpolar liquids.[20] This method is based on the (single) Mori formalism that separates the slow processes from the fast or quasi-instantaneous processes. The latter give rise to the decay of some TCFs (such as the molecular dipole moment's) so that at some order of separation, the Markovian approximation is justified.[21,22] The frequency dependent absorption coefficients from 0.1 to nearly 4.0THz

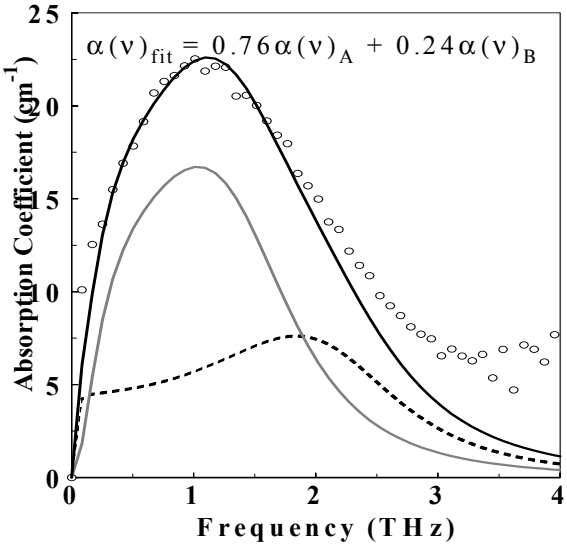

Figure 4: Bi-Mori fit (bold line) to the frequency dependent absorption coefficient spectrum for neat $CHCl_3$ (circles). The dashed (A) and solid gray (B) lines represent the Mori line shapes that compose the Bi-Mori line shape.

(3.3 to 134 cm^{-1}) of neat $CHCl_3$, two Mori curves and the bi-Mori fit are presented in Figure 4. The absorbance spectra for $CHCl_3$, CCl_4 and their mixtures (not shown) were fit by third order truncations of Mori's continued fraction, equivalent to a second order memory function analysis. When the spectra are fit with a four parameter non-linear least squares routine, the theoretical and experimental curves are nearly overlapped. However, when the adjustable parameters are constrained in a physically meaningful way and nonlinear least squares fitting is performed by varying only one parameter, the exponential relaxation time constant of the intermolecular torques, the fits to the experimental data for pure chloroform (as well as for CCl_4 and the mixtures) are quite poor.[20] This result indicates that a single Mori function, hence, single type of relaxation process, is not appropriate for chloroform or the mixtures.

Figure 4 illustrates the fit of the sum of the two single Mori functions to the data. Curve A (solid gray) uses Mori parameters that describe diffusive molecular motions and curve B (dashed) uses Mori parameters that describe inertial motions. The first order memory function related to the angular velocity time correlation function, in curve B is more inertial than in curve A. Furthermore, two parameters associated with torque relaxation are used: τ_D (in curve A) which describes rotational diffusion and τ_L (in curve B) which is smaller in value. The "bi-Mori" fit suggests that two (or more) types of molecular motion are necessary to describe the FIR spectrum of the liquid.

The assumption of exponential decay of the intermolecular torque correlation function is implicit in the third order truncation of the Mori continued fraction;[23] an assumption that may not be physically or rigorously correct. The theory should succeed at frequencies small relative to the torque decay rate. This prediction originates in the fundamental aim of Mori theory: the generation of a TCF for an observable variable. The premise is that other variables whose time correlation functions decay on comparable time scales cause the observable to behave in a non-Markovian way. In the present case, the two secondary variables, related to the first and second derivatives of the primary variable (*i. e.* the dipole moment), are closely related to the angular momentum and the intermolecular torque, respectively. For frequencies much less than the torque decay rate, the fastest process explicitly treated, the torque decay should seem instantaneous, and the line shape should describe experimental data well. The torque decay rate in Figure 4 is 12.5THz for both curves A and B. Hence for frequencies less than 15% of the torque decay rate (*i.e.* 2THz and below) the fit is of high quality, and the expected condition is observed.

4.2 HCl solvated in CCl_4

The THz time-domain waveforms for HCl/CCl_4 solutions are measured in transmission mode. The dilute solution of HCl in CCl_4 is prepared by bubbling HCl(g) into liquid CCl_4. The solution is transferred to a 1cm sample cell with silicon windows for measurement. The HCl/CCl_4 - pure CCl_4 frequency dependent absorption coefficient is shown in Figure 5 as the hollow circles. The structured spectrum along the baseline is that for HCl(g) measured in the same sample cell at ~1atm pressure.

The spectral theory[24] used here determines the FIR dipolar absorption spectrum to be a superposition of spectrally broadened and shifted rotational transitions ($\Delta j=\pm 1$) of a quantum rigid rotor. The magnitudes of these widths and shifts are ultimately determined by the anisotropic potential time auto-correlation function (APTAF). Although on average the solution is isotropic, the anisotropic intermolecular potential is important because anisotropy in the orientational fluctuations of the HCl molecules is determined by the interaction

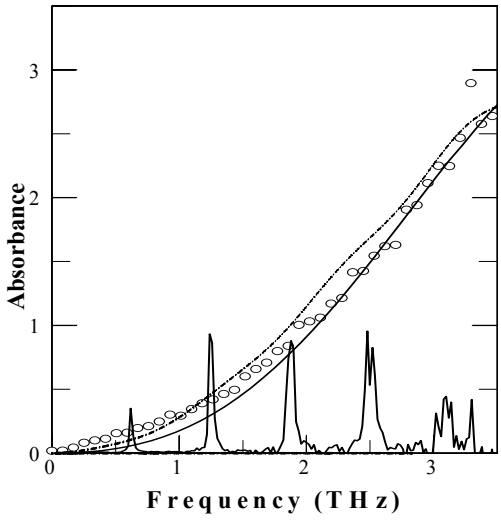

Figure 5: The absorbance spectrum of solvated HCl (hollow circles) is fit by a classical theory based on an MD generated rotational TCF (dashed line) and by a quantum mechanical rigid rotator based theory (solid line). The absorbance spectrum of gaseous HCl is shown as well (bold line).

between the HCl dipole and the surrounding solvent molecules. These solute-bath interactions are responsible for the rotational line broadening and shifting observed in the experimental spectra.[25]

The APTAF may be determined from molecular dynamics trajectories of the system and bath and experimentally determined anisotropic potential parameters from gas phase microwave and radio frequency spectra.[26] For the HCl/CCl_4 case, however, the van der Waals interactions have not been characterized; hence, a stochastic model is employed that requires only two fitting parameters.[27] At high densities the stochastic TCF (i.e. APTAF) exhibits an exponential decay, and has been shown to approximate the time scale of the decay and shape of the simulated correlation function reasonably well.[28]

The calculated fit normalized to the experimental data is shown as the solid line in Figure 5. A best fit was obtained when the interaction strength parameter λ_{red}^2=165 and the APTAF decay time τ_{red}=0.10 (in reduced units where $\lambda^2_{red}=\lambda^2_{fit}/(Bhc)^2$ and $\tau_{red}=(2\pi Bc)\tau_{fit}$).[25] In these formulas, B represents the rotational constant, h is Planck's constant and c denotes the speed of light. These results are qualitatively consistent with FT-IR spectra and simulations of HCl in Ar and SF_6. While CCl_4 is most similar in mass to SF_6, its polarizability of 11.2 is almost twice the value of SF_6 and seven times the value for Ar. A larger solvent polarizability means that the dipolar solute induces a proportionally larger dipole moment on the neighboring solvent molecules. Hence, the dipole-induced dipole interaction between HCl and CCl_4 is stronger than between HCl and SF_6 and much stronger than between HCl and Ar. This trend suggests that the stronger the dipole-induced dipole interaction in the solution, the greater the degree of line broadening and shifting in the corresponding absorption coefficient spectrum. Furthermore, the nature of intermolecular interaction between HCl and its CCl_4 bath neighbors is dominantly characterized by dipole-induced dipole associations.

5. Time Resolved THz Probe Studies of Solids

The optical pump–THz probe data illustrated in Figure 6a is the transient THz transmission for a 450μm thick wafer of undoped <111> GaAs recorded as a function of time following optical pump pulse excitation at 800nm. The data are recorded with the optical gating beam at the maximum amplitude of the THz pulse; the time axis refers to the pump–probe delay time obtained by scanning the optical beam delay stage (see Figure 2). Reduced transmission of the probe beam occurs due to the pump-induced sample absorbance of THz frequencies by the photo-generated carriers. An upper limit for the photo-excited carrier density corresponding to a 16nJ pulse, a focused beam diameter of 1mm and an assumed penetration depth of 126nm is estimated to be 1.3 $\times 10^{18}$ carriers/cm.[3] This data was detected in a double beam modulation scheme, in which both the pump beam and the THz source excitation beam were chopped. This step is necessary because rectification of the optical pump by the <111> GaAs sample causes a

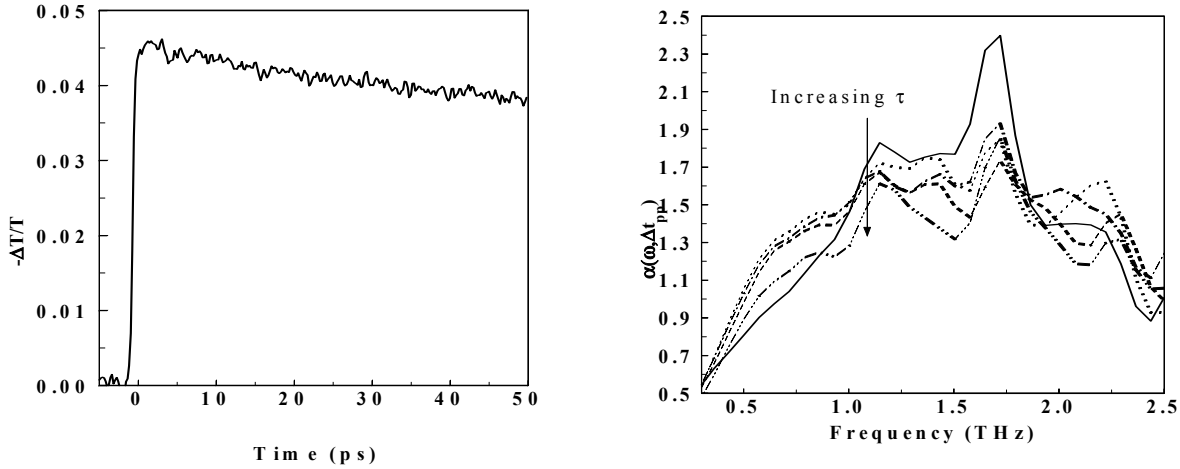

Figure 6: a) Optical pump-THz probe differential transmission data (a) and frequency domain absorbance data (b) obtained at several pump-probe delay times: bold 0.0ps, dotted 5.0ps, dot-dashed 10.0ps, dashed 20.0ps, dot-dot-dot-dashed 50.0ps.

contaminating second THz pulse to be incident on the receiver. This step, however, reduces the signal level by roughly a factor of three, so the signal-to-noise ratio is considerably reduced. Figure 6a also indicates the 4.5% modulation depth of the optically induced response. The S/N ratio of 83 demonstrates the high sensitivity of this apparatus. The slow decay of the signal is likely due to the carrier cooling dynamics.

Figure 6b illustrates the time dependent absorbance spectra obtained at various probe delay times. These data are referenced to the steady-state absorption coefficient spectrum for the measured GaAs sample. The spectra should be zero when pump-initiated events do not give rise to absorption and the probe frequencies that are absorbed are just those of the steady-state spectrum. Two relaxation processes are apparent in this series of data. Between 0.4 and 0.8THz the fast enhanced absorption (between 0.0 and 5.0ps) followed by slow diminishment in absorbance amplitude is consistent time scales observed for intervalley scattering of carriers.[29] That is, enhanced absorption occurs when carriers relax out high mobility valleys back into valleys characterized by lower carrier mobility and, therefore, higher absorption. The 1.0-1.7THz spectral region exhibits a monotonic decay of induced absorbance. This decay is consistent with the decreasing $-\Delta T/T$ signal with increasing pump-probe delay time illustrated in Figure 6a. This slower decay is likely due to carrier cooling via electron-phonon interactions, but since the exciton binding energy in GaAs is about 1THz,[29] there may be spectral contributions from exciton formation or relaxation dynamics. The ability to attain spectrally-resolved data makes these rather weakly-induced dynamics observable, and, thereby testifies to the sensitivity of the current instrument. A preliminary account of this research on free carrier dynamics was given elsewhere.[30]

6. Conclusions

The discussion carried out in this review leads to two observations on the optical pump-THz probe measurement of solvent reorganization. From an experimental point of view, high signal-to-noise ratios are essential to detect small induced absorbances. As the signal depends on the number of solvent molecules reorganizing, it is clear that increasing the concentration of solute molecules, increasing the intensity of the optical pump pulse, and choosing a solute molecule with a large dipole moment change upon excitation would increase the degree of solvent reorganization on a per shot basis. However, solute-solute interactions would contaminate the bath response signal, so massive solute concentrations are to be avoided. Multi-photon absorption in the solute might occur with optical pulses that are too intense, but this problem could be mitigated by looser focusing. As illustrated in Section 2, a large dipole moment change invalidates the assumption that the perturbation by the solute on the solvent is small. This issue of linear response, however, might be checked in a straight-forward way by observing the evolving induced spectrum at various time delays following optical excitation of the solute. Even in the event that it is found to fail for in a particular system, a quantitative upper bound for the allowed magnitude of the perturbation would be established. Still, optical pump-THz probe spectroscopy would be a more illustrative probe of linear response behavior than fluorescence Stokes-shift measurements.

7. Acknowledgements

We thank the NSF (CHE-9357424), the David and Lucile Packard, Camile Dreyfus and Alfred P. Sloan Foundations for financial support of the research.

8. References

[1] D. A. McQuarrie, *Statistical Mechanics*, Chapter 20, Harper Collins Publishers, New York, 1976.

[2] E. W. Castner, Jr. M. Maroncelli and G. R. Fleming, "Subpicosecond resolution studies of solvation dynamics in polar aprotic and alcohol solvents," *J. Chem. Phys.*, **86**, pp. 1090-1097, 1987.

[3] G. van der Zwan and J. T. Hynes, "Time dependent fluorescence solvent shifts, dielectric friction and non-equilibrium solvation," *J. Phys. Chem.* **89**, pp. 4181-4188, 1985.

[4] M. Maroncelli, "Computer simulation of Solvation Dynamics in Acetonotrile," *J. Chem. Phys*. **94**, pp. 2084 2103, 1991.

[5.] D. Chandler, *Introduction to Modern Statistical Mechanics*, Chapter 8, Oxford University Press, New York, 1987.

[6] Y. J. Yan and S. Mukamel, "Electronic dephasing, vibrational relaxation, and solvent friction in molecular nonlinear optical line shapes," *J. Chem. Phys.* **89**, pp. 5160-5176, 1988.

[7] M. Cho, S. J. Rosenthal, N. F. Scherer, L. D. Ziegler and G. R. Fleming, "Ultrafast solvation dynamics: connection between time-resolved fluorescence and optical Kerr measurements," *J. Chem. Phys.*, **96**, pp. 5033-5038, 1992.

[8] W. P. Deboeij, M. S. Pshenichnikov and D. A. Wiersma, "System-bath correlation function probed by conventional and time-gated stimulated photon echo," *J. Phys. Chem.*, **100**, pp. 11806-11823, 1996.

[9] It is unusual to refer to a ground state as a non-equilibrium state since the molecules spends most of it's time there; however, the solute is only used here as a device for changing the electric field at a precisely defined time, not as a subject of intrinsic interest.

[10] G. Haran, W. D. Sun, K. Wynne and R. M. Hochstrasser, "Femtosecond far-infrared pump-probe spectroscopy: A new tool for studying low-frequency vibrational dynamics in molecular condensed phases," *Chem. Phys. Lett.* **274**, pp. 365-371, 1997.

[11] R. McElroy and K. Wynne, "Ultrafast dipole solvation measured in the far-infrared," *Phys. Rev. Lett.*, **79**, pp. 3078-3081, 1997.

[12] M. C. Nuss, D. H. Auston and F. Capasso, "Direct subpicosecond measurement of carrier mobility of photoexcited electrons in gallium arsenide," *Phys. Rev. Lett.*, **58**, pp. 2355-2358, 1987.

[13] B. I. Greene, J. F. Federici, D. R. Dykaar, A. F. Levi and L. Pfeiffer, "Picosecond pump and probe spectroscopy utilizing freely propagating terahertz radiation," *Opt.Lett.*, **16**, pp. 48-49, 1991.

[14] R. M. H.Groenveld and D. Grischkowsky, "Picosecond time-resolved far-infrared experiments on carriers and excitons in GaAs-AlGaAs multiple quantum wells," *JOSA B,* **11**, pp. 2502-2507, 1994.

[15] B. B. Hu, E. A. Souza, W. H. Knox, J. E. Cunningham, M. C. Nuss, A. V. Kuznetsov and S. L. Chuang, "Identifying the distinct phases of carrier transport in semiconductors with 10fs resolution," *Phys. Rev Lett.*, **74**, pp. 1689-1692, 1995 .

[16] B. N. Flanders, D. C. Arnett and N. F. Scherer, "A cavity-dumped oscillator-driven terahertz spectrometer for optical pump-THz probe spectroscopy," *IEEE JQE: Special Issue on Ultrafast Optics*, in review, 1997.

[17] D. C. Arnett, M. A. Horn and N. F. Scherer, "Femtosecond and two color nonlinear spectroscopy with a cavity-dumped ti:sapphire oscillator," *SPIE Technical Program*, Submitted December, 1997.

[18] N. Katzenellenbogen and D. Grischkowsky, "Efficient generation of 380fs pulses of THz radiation by ultrafast laser pulse excitation of a biased metal-semiconductor interface," *Appl. Phys. Lett.*, **58**, pp. 222-224, 1991.

[19] Q. Wu, M. Litz and X. C. Zhang, "Broadband detection capability of ZnTe electro-optic field detectors," *Appl. Phys. Lett.*, **68**, pp. 2924-2926, 1996.

[20] B. N. Flanders, R. A. Cheville, D. Grischkowsky and N. F. Scherer, "Pulsed terahertz transmission spectroscopy of liquid $CHCl_3$, CCl_4 and their mixtures," *J. Phys. Chem.*, **100**, pp. 11824-11835, 1996.

[21] H. Mori," A continued fraction representation of the time-correlation functions," *Prog. Theor. Phys.*, **34**, pp.399-416, 1965.

[22] H. Mori, "Transport, collective motion, and Brownian motion" *Prog. Theor. Phys.*, **34**, pp.423-454, 1965.

[23] D. Kivelson and P. Madden, "A molecular treatment of dielectric phenomena," *Adv. Chem. Phys.*, **56**, pp. 480-566, 1984.

[24] S. Mukamel, "Non-Markovian theory of molecular relaxation I. Vibrational relaxation and dephasing in condensed phases*," Chem. Phys*., **37**, pp. 33-47, 1978.

[25] B. N. Flanders, P. Moore, M. L. Klein, D. R. Grischkowsky and N. F. Scherer, "Pulsed terahertz, molecular dynamics simulation and analytical study of a simple solution: HCl in CCl_4," To be submitted to *J. Chem. Phys.*, 1998.

[26] S. L. Holmgren, M. Waldman and W. Klemperer, Internal dynamics of van der Waal complexes I. Born-Oppenheimer separation of radial and angular motion, *J. Chem. Phys.*, **67**, pp. 4414-4422, 1977.

[27] A. Medina, S. Velasco, A. C. Hernández, "Quantitative study of memory and nonadditivity effects the far-infrared spectrum of HCl in dense Ar," *Phys. Rev A*, **44**, pp. 3023-3031, 1991.

[28] A. Medina, A. C. Hernández and S. Velasco, "Far-infrared spectrum of HCl in dense Ar and time-dependent anisotropic potential autocorrelation function: A molecular dynamics study," *J. Chem. Phys*., **100**, pp. 252-261, 1994.

[29] C. Kittel, *Introduction to Solid State Physics*, 7th Edition, John Wiley &Sons: New York, 1996.

[30] B. N. Flanders and N. F. Scherer, *Ultrafast Phenomena XI*, W. Zinth, J. Fujimoto, T. Elsaesser, D. Wiersma, Eds.; Springer Series in Chemical Physics, Springer-Verlag: Berlin, 1998, submitted.